Transport Properties of Bulk-Bicrystal Grain Boundaries in Artificially Joined Large-Grain YBCO

A. D. Bradley, R. A. Doyle, D. Charalambous, W. Lo, D. A. Cardwell, A. M. Campbell
IRC in Superconductivity, University of Cambridge, Madingley Road, Cambridge CB3 0HE, U.K.

Ph. Vanderbemden
SUPRAS, Montefiore Electricity Institute B28, University of Liege, Sart-Tilman, B-4000 Liege, Belgium

***Abstract*—A technique for joining large-grain YBCO has been used to produce bulk-bicrystal grain boundaries of different orientations. The behaviour of boundaries nominally of 0°[100], 0°[001] and asymmetric 15°[100]-tilt misorientation have been investigated using low frequency transport measurements in fields up to 7 T. The boundaries exhibit a metallic normal state and a superconducting transition which broadens with increasing field having an irreversibility line which closely matches that of the adjoining grains. This same qualitative behaviour is seen in all the samples measured for field applied parallel and perpendicular to the c-axis and up to the highest current densities employed ($20\,A cm^{-2}$). Variation between the different samples due to microstructural differences are discussed. We interpret these results as strong suggestive evidence that this joining technique can be used to produce strongly-coupled large-grains for bulk-scale engineering applications.**

I. Introduction

The development of large-grain (RE)BCO materials has generated wide interest in the potential use of superconductors in bulk-scale engineering applications which require large magnetic fields. The details of preparation of such materials and limiting factors in their growth are discussed in [1] and [2]. It is clear that production of samples larger than a few cm will be more easily enabled by joining technologies than by changes in the growth technique. Thus the properties of artificial grain boundaries in these materials are of considerable interest. Although clean well-defined (non-meandering) grain boundaries can be produced in large-grain YBCO using a dual-seeding technique [3] and some other joining experiments have been carried out [4]–[6], there is surprisingly little general research in this area, given its potential technological importance. Several important differences exist between the current carrying ability of bulk-bicrystal grain boundaries compared to those in thin films [7]. Some differences may be expected because bulk samples are always much thicker than expected Josephson penetration depths [8] while meandering in thin film boundaries may lead to increased pinning of Josephson vortices [9]. In general however much work remains to be done to understand fully the behaviour of bulk grain boundaries.

Manuscript received September 14, 1998.
A. D. Bradley, +44 1223 337049, fax +44 1223 337074, adb30@cam.ac.uk. This work was supported by EPSRC. Ph.V. is grateful to FNRS for a research grant.

In this study we have performed transport measurements on large-grain YBCO joined using the technique developed by Lo et al. [2]. We discuss their behaviour in terms of the artificial grain boundary which is created at the interface.

II. Experimental

Large grains of melt-processed $YBa_2Cu_3O_{7-\delta}$ were joined and re-oxygenated following the technique described in [2]. Fig. 1 shows schematically the different joins used in this study and the direction of transport current flow, J. The 0°[100] and 0°[001] boundaries will here-in be denoted ab^0 and c^0 respectively and the asymmetric 15°[100]-tilt boundary, ab^{15}. The typical sample size after joining was $2\,cm^3$. Several samples of approximate dimension 2 mm × 0.5 mm × 0.3 mm were cut from each large piece and finely polished (0.25 μm) to reveal the microstructural features. The grain orientation was confirmed optically by observing the misorientation of platelets and in the case of the zero-angle boundaries the continuity of twin boundaries in crossing the artifi-

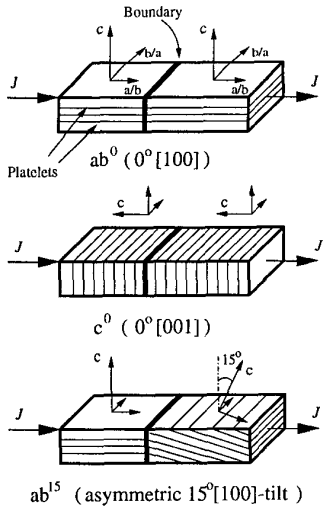

Fig. 1. Schematic of the artificial grain boundary geometries. The direction of current flow, J, is labeled along with the platelets (parallel to the ab-planes) and c-axes in each grain. The actual sample orientations have been found to be within 3° of these nominal values as determined by optical and X-ray measurements.

cial boundary. Samples free from visible microcracks and containing only minimal amounts of liquid phase at the boundary [2] were selected for transport measurements. At least two samples of each boundary type have been measured to confirm the generality of our conclusions.

In addition one of the ab^0-joined samples which had previously been shown to have intimate coupling between the grains [10] was thinned to $\sim 50\,\mu$m and cut into bars of width $\sim 100\,\mu$m using a miniature wire saw. This enabled higher current densities to be obtained without the need for large currents which can lead to ohmic heating at the contacts.

Four-point electrical contacts with a specific contact resistance of $\sim 10^{-3}\,\Omega\text{cm}^2$ were made to all the samples [11]. Voltage contacts on either side of the boundary in both grains (see Fig. 2 inset) allowed the resistance across the boundary as well as in the grains to be measured simultaneously. This was carried out with nanovolt resolution using a 72 Hz current source and lock-in amplifiers with low-noise transformers. A goniometer stage on the sample probe allowed the accessible fields (up to 7 T) to be applied either parallel to the ab-planes or the c-axis of either grain. In addition isothermal magnetization measurements were made on individual grains using a Quantum Design SQUID magnetometer.

III. Results

Fig. 2 shows the field-dependent broadening of the resistive transition in one grain (G1) and across the boundary (GB) for a thinned ab^0 sample with current density, $J \approx 20\,\text{Acm}^{-2}$. The applied field direction, H_a was parallel to the c-axis as shown in the inset. The grain transition is sharp in zero field and broadens with increasing field as is usually observed in HTS. The transition for the other grain (G2) was identical apart from a small difference in T_c of 0.3 K (see below). At temperatures below that at which the grains adjoining the GB become superconducting the GB resistance shows a distinct "foot" for $R < 10^{-3}\,\Omega$ which is due to the GB normal state resistance, R_N. This indicates metallic behaviour with positive dR_N/dT. At lower temperatures the resistance of the GB falls below our sensitivity. The broadening of the GB transition follows very closely that of the grains, the main difference being a shift in T_c of about 2.5 K (the data for the GB are weakly non-linear so this estimate is an upper bound). The behaviour with $H_a//\text{ab}$ is qualitatively the same except that the transitions for the grains and GB are shifted to higher temperatures as expected from the anisotropy of the material.

The resistive transitions for the grains and GBs in samples of all three join configurations shown in Fig. 1, all with similar cross-sections, are presented for comparison in Fig. 3 with $J \approx 0.5\,\text{Acm}^{-2}$. The applied field was 0.4 T parallel to the c-axis in all cases except the sample ab^{15} where it lies at 15^o to the c-axis in one of the grains. The transitions are plotted in terms of the resistance-area product ($R_{GB}A$) so as to effectively compare the GB normal state resistivities (strictly speaking the GB resistivity multiplied by the width of the disordered GB region). For clarity, the grain resistance is normalised to R_{GB} above T_c where it is dominant. Measurements on two samples of each type show that the broadening of the GB transition in the c^0 sample is larger than for ab^0 while that of ab^{15} is intermediate between the other two. Note that in the c^0 sample $H_a//J$ but the resistivity broadening in the grains was no different to that in the other samples, so no Lorentz "force-free" effects were apparent [12]. The R_NA values for the ab-joined samples here are higher than those of thin-film bicrystals which lie in the range $10^{-1} - 10^{-3}\,\mu\Omega\text{cm}^2$ [13], although we have found values as low $6 \times 10^{-2}\,\mu\Omega\text{cm}^2$ in some samples from the same starting material [10]. We believe these differences to be due to variations in the effective boundary contact area caused by liquid phase trapped at the boundary [2]. Significantly, the c^0 sample has an R_NA value which is larger than the

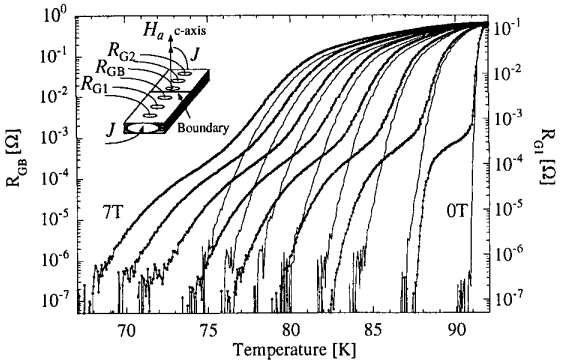

Fig. 2. Resistance measured in one grain, R_{G1} (solid lines) and across the grain boundary, R_{GB} (marked by points) as a function of temperature for a thinned ab^0 sample with current density $J \approx 20\,\text{Acm}^{-2}$. Applied field, $\mu_0 H_a$ was 0, 1, 2, 3, 4, 5, 6 and 7 T parallel to the c-axis, as shown in the inset.

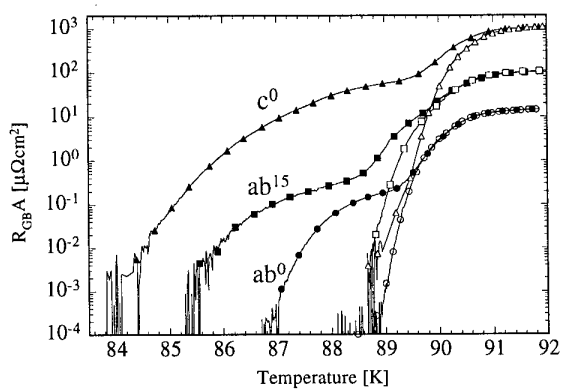

Fig. 3. The temperature dependence of the resistance-area product, $R_{GB}A$, where A is the whole sample-cross section for the three different joined samples: ab^0 (circles), ab^{15} (squares) and c^0 (triangles). The applied field was 0.4 T parallel to the c-axes and the current density was $\sim 0.5\,\text{Acm}^{-2}$. The resistance of the grains (open symbols) is normalised to R_{GB} above T_c.

ab-joined samples by a factor of about 150 and cannot therefore be accounted for by the resistivity anisotropy alone ($\rho_c/\rho_{ab} \approx 30-60$ in the grain material). Note that the behaviour in Fig. 3, and in particular the differences between the samples, does not change qualitatively with either field or current.

A "resistive irreversibility line", IL_R, for the grain and GB in each of these three samples has been extracted from the resistance-temperature data (measured with $J \approx 0.5 \mathrm{Acm}^{-2}$) using a criterion of $5 \times 10^{-7}\,\Omega$. The inset to Fig. 4(a) shows the IL_R for the sample ab^0. Also shown is a "magnetic irreversibility line" for the grain material extracted from magnetisation hysteresis loops at different temperatures using a criterion of $25\,\mathrm{Acm}^{-2}$. The irreversibility field, H_{irr}, for the grain and GB in all three samples was found to fit a power-law dependence, $H_{irr} = H_0(1 - T/T_c)^{4/3}$, as found for the irreversibility and melting lines in YBCO single crystals [14]. The values of the fit parameters obtained for each of the samples are given in Table I. In order to allow easier comparison between the IL's for the three types of grain boundary we have normalised the irreversibility field of each sample to the value of the grain irreversibility field, H_{irr}^{Gr}, at 76 K and 87 K for $H_a//c$ and $H_a//ab$, respectively. This construction is shown in Fig. 4(a) for fields applied parallel to the c-axis and (b) for fields parallel to the ab-planes. The data are also plotted as a function of reduced temperature, T/T_c, where T_c corresponds to that of the grain. This allows us to account for small variations in T_c within the grains of different samples. These arise from variations in cation content in the samples from different positions relative to the seed crystal in the original large-grain [15]. Fig. 4(a) shows that the trend in the behaviour of the three boundaries shown in Fig. 3 for $H_a = 0.4\,\mathrm{T}$ persists for all fields up to 7 T. The IL_R of sample ab^0 follows that of the grains very closely while for samples ab^{15} and c^0 the differences between grain and GB grow slowly with increasing field. Similar behaviour is seen in Fig. 4(b) for $H_a//ab$, except that the IL's of c^0 and ab^{15} lie closer to one another.

TABLE I

Fit parameters to the relation $H_{irr} = H_0(1 - T/T_c)^{4/3}$ for the resistive irreversibility lines in all three samples.

		GB		Grain	
	Sample	$\mu_0 H_0$[T]	T_c[K]	$\mu_0 H_0$[T]	T_c[K]
$H_a//c$	ab^0	80	89.8	88	91.2
	ab^{15}	56	87.5	75	90.3
	c^0	48	87.0	80	91.0
$H_a//ab$	ab^0	550	89.5	500	91.0
	ab^{15}	260	87.5	500	91.0
	c^0	270	86.5	480	90.8

IV. Discussion

The data in Figs. 4(a) and (b) show that the irreversibility lines for all the artificial grain boundaries lie

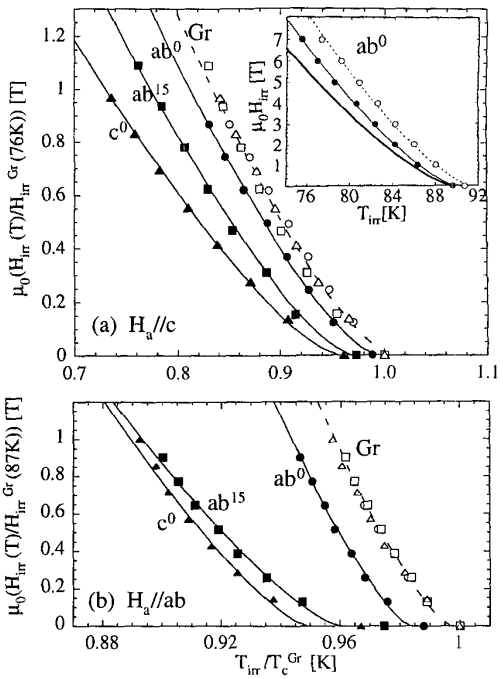

Fig. 4. Resistive irreversibility lines IL_R for the grains (open data points) and GB's (solid data points) in the three samples: ab^0 (circles), ab^{15} (squares) and c^0 (triangles). The irreversibility fields, H_{irr}, are scaled to H_{irr} for each grain at 76 K for $H_a//c$ (a) and at 87 K for $H_a//ab$ (b). The reduced temperature axis is scaled to the T_c of the grains. The curves are fits to the power law relation $H_{irr} = H_0(1 - T/T_c)^{4/3}$, the values for which are given in Table I. The inset in (a) shows the IL_R for grain (open circles) and GB (closed circles) in sample ab^0 along with a "magnetic IL" for the grain material (solid curve).

fairly close to those of the grains themselves. This is in marked contrast to what is expected from "weakly linked" boundaries (e.g. most high-angle natural bulk-bicrystal boundaries) where a pronounced field dependence is observed, even in fields of order mT [7], [11]. The slightly reduced T_c for all the grain boundaries here may be due to lattice strain, cation contamination, or to a difference in the requirements for optimum oxygenation in grain and boundary and requires further detailed micro-chemical and microstructural analysis. Furthermore, the thinned sample in Fig. 2 exhibits a lower T_c for the boundary than the thicker sample from which it was cut. We are as yet unable to determine whether this is due to damage occuring during sample preparation, or to microstructural inhomogeneity along the joined boundary. The IL_R which we define indicates an upper bound for the temperature at which the critical current of the sample becomes equal to the applied current. This is confirmed by the data in the inset of Fig. 4(a) where the magnetically determined IL (which gives a lower bound for the true onset of a critical current) is shown together with the IL_R for a grain in an ab^0 sample. Note that the criterion at which the IL_R is defined lies more than five orders of magnitude

below the normal state resistance of the grain, giving confidence that a critical current is developing. Ideally, the critical current should be evaluated in detail as a function of both field and temperature. For typical sample cross sections in this work, a critical current density of 10^4 Acm^{-2} would require application of ~30 A to the sample. Although we are able to achieve sub-ohmic contact resistance, this nonetheless incurs considerable joule heating and requires pulsed-current techniques. This work is in progress and we concentrate here on determining the maximum field-dependent temperatures at which the boundaries will carry supercurrent. In general, and as discussed above, bicrystals which have small critical currents frequently display a pronounced field dependence, contrary to what we observe here. The quality of all the boundaries is further suggested by their metallic normal state resistance. In the case of the ab^0 sample in particular, this is confirmed by recent TEM studies which show regions in which the recrystallised boundary is flat and almost perfect on an atomic scale [2].

Next we consider the differences between the different types of boundary. It is well known that the critical current of boundaries in YBCO thin films falls dramatically for tilt angles larger than about 10^o. In bulk bicrystals the trend is the same although not as pronounced [7]. It is therefore not surprising that the performance of sample ab^{15} is inferior to that of the ab^0 samples. On the other hand, the properties in this sample are not suppressed far below the ab^0 sample. Optical micrographs indicate that the boundary displays periodic faceting (on a scale of the platelet boundaries, i.e. ~1-5 μm) with the boundary intermittently parallel to each grain. We believe that the c^0 sample may be inferior to the ab^0 sample due to the role of the liquid phase which controls recrystallisation at the boundary. In the c^0 sample, optical micrographs reveal that considerable amounts of this phase are still present in the boundary. This is consistent with the enhanced R_N for the boundary and along with a contribution due to the critical current anisotropy ($J_c^{ab}/J_c^c \sim 10$ in the grains [11]) may account for the suppressed IL.

Finally, it is interesting to note that, in addition to the form of the irreversibility line, the anisotropy in the behaviour of the boundaries is very similar to that of the grain. This suggests that similar mechanisms may control the onset of dissipation in the grain and boundary and is in agreement with experiments which show that grain boundary critical current can be changed by changing that in the grains themselves [16].

V. Conclusion

We have measured the field dependence of the resistive transitions in artificial grain boundaries of three different orientations and found that the behaviour in all the samples is consistent with strong coupling between the grains. We conclude that this new joining process is promising for the production of bulk-scale high-field engineering applications requiring macroscopic supercurrent flow over length scales larger than those obtainable in individual large-grains.

Acknowledgment

We wish to thank J. Chrosch for X-ray diffraction work, E.J. Tarte for helpful discussions and E.S. Sadki for technical assistance.

References

[1] D. A. Cardwell, *Materials Science and Engineering*, vol. B53, pp. 1–10, May 1998.

[2] W. Lo, D. A. Cardwell, S. J. Lloyd, A. D. Bradley, R. A. Doyle, and Y. H. Shi, *IEEE Trans. Appl. Supercond.*, submitted to ASC'98.

[3] V. R. Todt, X. F. Zhang, D. J. Miller, M. St. Louis-Weber, and V. P. David, *Appl. Phys. Lett.*, vol. 69, no. 24, pp. 3746–3748, December 1996.

[4] K. Salama and V. Selvamanickam, *Appl. Phys. Lett.*, vol. 60, pp. 898–900, February 1992.

[5] Donglu Shi, *Appl. Phys. Lett.*, vol. 66, no. 19, pp. 2573–2575, May 1995.

[6] G. J. Schmitz, A. Tigges, and J. C. Schmidt, *Supercond. Sci. Technol.*, vol. 11, pp. 73–75, 1998.

[7] M. B. Field, D. C. Larbalestier, A. Parikh, and K. Salama, *Physica C*, vol. 280, pp. 221–233, April 1997.

[8] A. Gurevich and E. A. Pashitskii, *Phys. Rev. B*, vol. 57, no. 21, pp. 13878–13893, June 1998.

[9] K. E. Gray, M. B. Field, and D. J. Miller, *Phys. Rev. B*, vol. 58, no. 14, pp. 9543–9548, October 1998.

[10] R. A. Doyle, A. D. Bradley, W. Lo, D. A. Cardwell, A. M. Campbell, Ph. Vanderbemden, and R. Cloots, *Appl. Phys. Lett.*, vol. 73, pp. 117–119, July 1998.

[11] Ph. Vanderbemden, A. D. Bradley, R. A. Doyle, W. Lo, D. M. Astill, D. A. Cardwell, and A. M. Campbell, *Physica C*, vol. 302, pp. 257–270, 1998.

[12] K. Kadowaki, Y. Songliu, and K. Kitazawa, *Supercond. Sci. Technol.*, vol. 7, pp. 519–540, 1994.

[13] H. Hilgenkamp and J. Mannhart, *Appl. Phys. Lett.*, vol. 73, no. 2, pp. 265–267, July 1998.

[14] J. R. Cooper, J. W. Loram, J. D. Johnson, J. W. Hodby, and Chen Changkang, *Phys. Rev. Lett.*, vol. 79, no. 9, pp. 1730–1733, September 1997.

[15] C. D. Dewhurst, W. Lo, Y. H. Shi, and D. A. Cardwell, *Materials Science and Engineering*, vol. B53, pp. 169–173, May 1998.

[16] D. C. Larbalestier, unpublished.